

Electronic Journal of Polish Agricultural Universities is the very first Polish scientific journal published exclusively on the Internet, founded on January 1, 1998 by the following agricultural universities and higher schools of agriculture: University of Technology and Agriculture of Bydgoszcz, Agricultural University of Cracow, Agricultural University of Lublin, Agricultural University of Poznan, University of Podlasie in Siedlce, Agricultural University of Szczecin and Agricultural University of Wrocław.



**ELECTRONIC  
JOURNAL  
OF POLISH  
AGRICULTURAL  
UNIVERSITIES**

**2005  
Volume 8  
Issue 2  
Topic  
WOOD  
TECHNOLOGY**

Copyright © Wydawnictwo Akademii Rolniczej we Wrocławiu, ISSN 1505-0297

SMARDZEWSKI J. , OŻARSKA B. 2005. RIGIDITY OF CABINET FURNITURE WITH SEMI-RIGID JOINTS OF THE CONFIRMAT TYPE *Electronic Journal of Polish Agricultural Universities*, Wood Technology, Volume 8, Issue 2.

Available Online <http://www.ejpau.media.pl>

## **RIGIDITY OF CABINET FURNITURE WITH SEMI-RIGID JOINTS OF THE CONFIRMAT TYPE**

Jerzy Smardzewski<sup>1</sup>, Barbara Ożarska<sup>2</sup>

<sup>1</sup>*Department of Furniture Design, The August Cieszkowski Agricultural University of Poznań, Poland*

<sup>2</sup>*University of Melbourne, Australia*

### **ABSTRACT**

The objective of the experiment was to construct a mathematical model of a semi-rigid angle joint of the confirmat type and a numerical model of cabinet furniture construction with semi-rigid screw joints of the confirmat type. It was shown that models of a semi-rigid constructional node of the confirmat type describe well work of a rigid connector in the neighbourhood of strongly deformable wood-derived materials. In addition, the authors elaborated a mathematical and numerical model of a semi-rigid angle joint of the confirmat type loaded with a bending moment.

**Key words:** screw, chipboard, cabinet furniture, mathematical model, numerical model

### **INTRODUCTION**

Screw joints of cabinet furniture belong to a group of semi-rigid joints for which the entire rigidity of the entire system depends on the rigidity of all its component parts. The treatment of these joints in engineer calculation models as ideally rigid nodes seems to be overoptimistic and as articulated joints – exceptionally disadvantageous. Only semi-rigid models allow correct mathematical descriptions and numerical modelling of the constructional rigidity of cabinet furniture connected by means of screws.

### **OBJECTIVE OF THE RESEARCH PROJECT**

The aim of the study was to design a mathematical model of a semi-rigid angle joint of the confirmat type and to determine the distribution of stresses in the connected elements. The second aim of the study was to construct mathematical rigidity models of semi-rigid screw joints of the confirmat type, which were subjected to bending moments and to generate numerical models corresponding to these solutions.

## MATHEMATICAL MODEL OF SCREW JOINTS OF THE CONFIRMAT TYPE

From the investigations on the load-carrying ability of connectors of the confirmat type performed so far [1] it is evident that the mean pullout strength parallel to the wide surface of boards of the screw driven to the depth of 30 mm amounts to 1250N (Fig. 1).

**Fig. 1. Screw pullout strength parallel to the wide surface of the board (author's own elaboration after [1])**

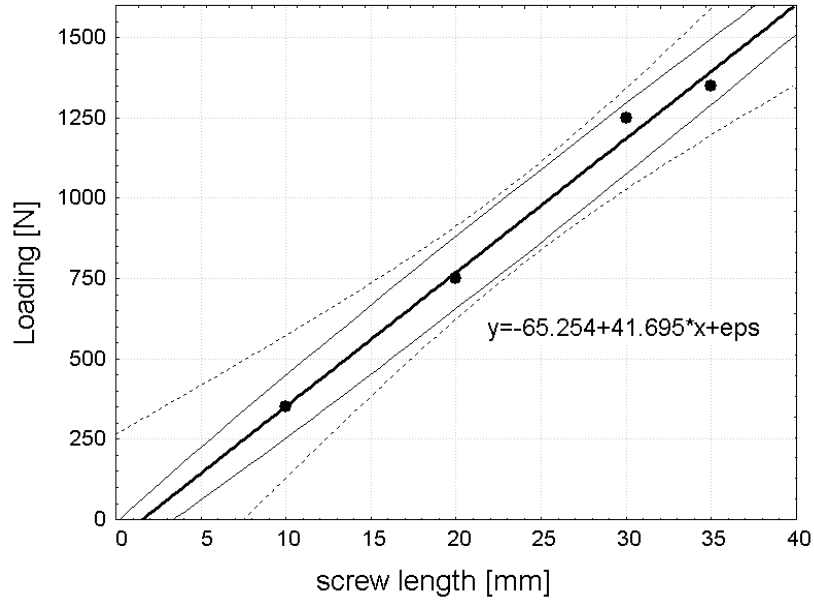
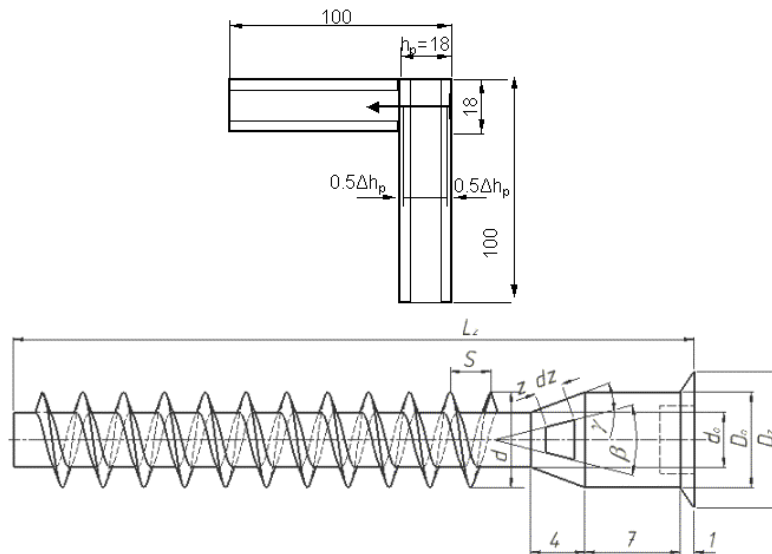


**Fig. 2. Dimensions of the screw and angle joint of the confirmat type**



Assuming this value as the force in the screw core and selecting screw geometric characteristics and material constants of a three-layer chipboard [2] (Table 1) for the angle joint as shown in Figure 2, impact cones were determined taking into account: only loads from the screw head (Fig. 3) or loads from the screw cone (Fig. 4). Next, successively, the following parameters were calculated:

- Screw rigidity coefficient  $c_s$ ,
- Board rigidity coefficient (flange)  $c_k$ ,
- Load coefficient  $\xi$ ,
- Joint initial stress  $Q_0$ ,
- Joint maximum stress  $Q_{max}$ ,

- Joint residual stress  $Q_r$ ,
- Screw driving moment  $M$
- Acceptable board compression caused by the initial screw stress  $\Delta h_p$ ,
- Maximum screw load  $P_r$  causing board contraction equal to  $\Delta h_p$ .

**Table 1. Mechanical properties of the chipboard [1,2]**

Property	Unit of measure	Value
$E_1$ Young's modulus of board external layers	MPa	4656
$E_2$ Young's modulus of board internal layer		1080
$E_s$ Young's modulus of steel		200000
$\nu$ Poisson's coefficient for all materials	-	0.3
$k_f^w$ Board ply adhesion strength	MPa	0.71
$k_t^w$ Board shear strength		5.35
$E_g$ Rigidity of the type GAP element		1080
$h_p$ Board thickness	mm	18
$h_1$ Thickness of the board outside layer		3
$h_2$ Thickness of the board inside layer		12
$L_z$ Length of screw		50
$l_i$ Height of the $i^{\text{th}}$ surface of the cone of impact		
$D_o=d$ Outer diameter of thread, diameter of cylinder part		7
$D_i$ Diameter of the $i^{\text{th}}$ surface of the cone of impact		
$D_z$ Outer diameter of the screw head		10
$d_o$ Diameter of the screw core		4
$\beta$ Angle of the elemental section of the friction surface	deg	
$\gamma$ Cone angle of the screw head		21
$A_i$ Area of the $i^{\text{th}}$ part of the cone of impact	$\text{mm}^2$	
$A$ Friction surface of the screw head cone		
$S$ – Pitch of thread	mm	3
$dz$ Width of the elemental section of the friction surface		
$M_f$ Moment of friction	Nmm	
$M_G$ Moment on the thread		
$N$ Load force	N	
$T$ Friction force		
$\mu$ Friction coefficient of board against metal	-	

**Fig. 3. Cones of impact from the pressure of the screw flange**

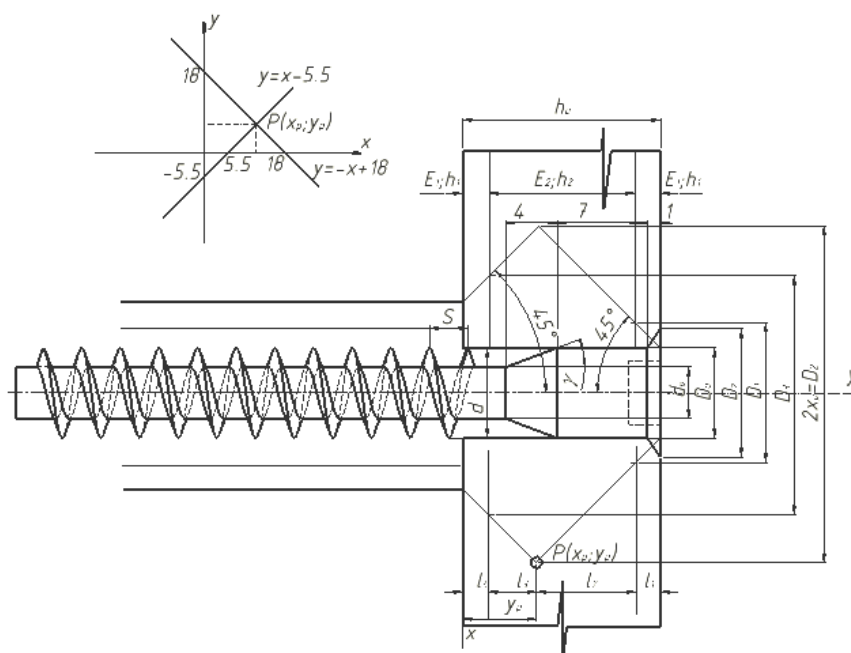
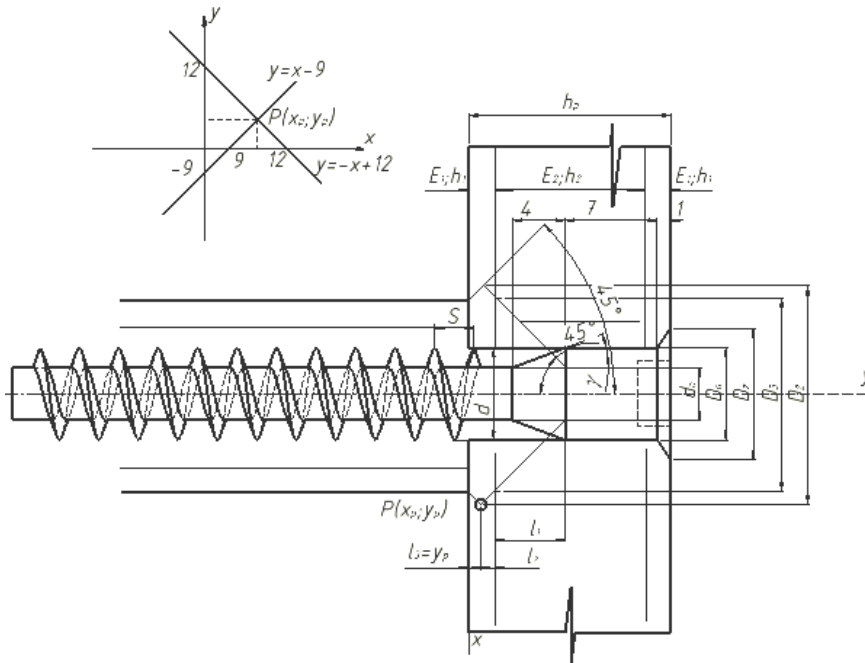


**Fig. 4. Cones of impact from the pressure of the screw cone**



The following parameters were obtained for the diagram from Figure 3:

$$c_x = \int_{x_1}^{x_2} \frac{1}{E_x A_x} dx,$$

$$\frac{1}{c_s} = \frac{4}{\pi E_s} \left( \frac{7}{D_o} + \frac{4 \cdot 4}{(D_o + d_o)^2} + \frac{18 - 7 - 4}{d_o^2} \right) = 4.5364796 \cdot 10^{-6} \left[ \frac{\text{mm}}{\text{N}} \right],$$

$$\frac{1}{c_k} = \frac{l_1}{E_1 A_1} + \frac{l_2}{E_2 A_2} + \frac{l_3}{E_2 A_3} + \frac{l_4}{E_1 A_4},$$

$$\frac{1}{c_k} = \frac{4h_1}{\pi E_1 ((D_o + h_1)^2 - D_o^2)} + \frac{4(h_p - h_1 - y_p)}{\pi E_2 ((D_o + h_1 + x_p)^2 - D_o^2)} + \frac{4(y_p - h_1)}{\pi E_2 \left( \left( \frac{D_o + 2x_p + h_p + 2h_1}{2} \right)^2 - D_o^2 \right)} + \frac{4h_1}{\pi E_1 ((h_p + h_1)^2 - D_o^2)} = 4.803085 \cdot 10^{-5} \left[ \frac{\text{mm}}{\text{N}} \right]$$

$$\zeta = \frac{c_s}{c_s + c_k} = 0.913,$$

$$Q_o = Q(1 - \zeta)k_z = 129.36\text{N}; \quad Q_{\max} = Q_o + \zeta Q = 1270.6\text{N}; \quad Q_r = Q_{\max} - Q = 20.6\text{N}.$$

The value of the shortening  $\Delta h_p$  of the vertical element of the joint caused by the maximum force  $Q_{\max}$  derived from the initial assembly equals:

$$\Delta h_p = Q_{\max} \left( \frac{l_1}{E_1 A_1} + \frac{l_2}{E_2 A_2} + \frac{l_3}{E_2 A_3} + \frac{l_4}{E_1 A_4} \right) = 0.061\text{mm}.$$

On the other hand, for the diagram from Fig. 4, the following were obtained:

$$\frac{1}{c_s} = \frac{4}{\pi E_s} \left( \frac{4}{\left( \frac{D_o + d_o}{2} \right)^2} + \frac{6}{d_o^2} \right) = 3.229 \cdot 10^{-6} \left[ \frac{\text{mm}}{\text{N}} \right],$$

$$\frac{1}{c_k} = \frac{l_1}{E_2 A_1} + \frac{l_2}{E_1 A_2} + \frac{l_3}{E_1 A_3} = 5.9 \cdot 10^{-5} \left[ \frac{\text{mm}}{\text{N}} \right],$$

$$\zeta = 0.9484,$$

$$Q_o = 77.25 \text{ N}; Q_{\max} = 1262.86 \text{ N}; Q_r = 12.86 \text{ N},$$

$$\Delta h_p = 0.0885 \text{ mm}.$$

In order to construct a numerical model, the calculation model as shown on Figure 4 and the value of the force  $Q_{\max} = 1262.89 \text{ N}$  were selected. Taking also into consideration friction forces on the screw cone and thread (Fig. 5), the value of the tightening moment  $M$  was determined which equaled:

$$M = M_T + M_G$$

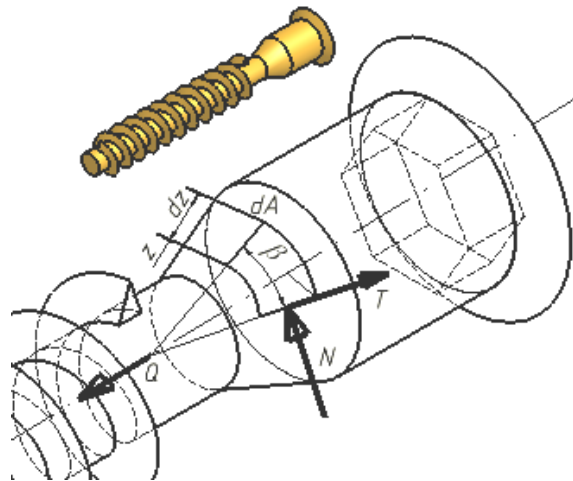
where:

$$M_T = \mu \frac{4 \sin \gamma Q_o}{(\mu \cos \gamma + \sin \gamma)(D_o^2 - d_o^2)} \sin \gamma \int_{\frac{d_o}{2 \sin \gamma}}^{\frac{D_o}{2 \sin \gamma}} z^2 \int_0^{2\pi} dz d\beta,$$

$$M_G = \frac{1}{2} Q_{\max} D_o \operatorname{tg} \left( a \operatorname{tg} \frac{S}{\pi D_o} + a \operatorname{tg} \mu \right),$$

$$M = 18646.9 [\text{Nmm}].$$

**Fig. 5. Internal screw forces**



When developing the numerical model of the described joint of the confirmat type (Fig. 6), the effect of compression of the vertical board was simulated by the compression of the non-threaded part of the screw set in the  $h_p$  interval by force  $P_r = 24714.76 \text{ N}$  causing the contraction of the core  $\Delta h_p = 0.0885 \text{ mm}$ .

The distribution of reduced stresses after Mises (Fig. 7) indicates that the strongest efforts of the chipboard developed in the part compressed by the screw head and the horizontal element. The stresses were small along the threaded part of the screw and they did not influence the destruction of the material of the inner board layer.

Mathematical and numerical solutions presented upper, comprised a case when a connector was loaded with axial assembly forces  $Q_{\max}$ . In practical conditions of cabinet furniture design, much more complex states of

loads affect their nodes. Bending moments, which cause mutual stresses of joint elements, belong to the most dangerous ones. Deformations of the connector as well as distortions of board elements cause that the rigidity of the constructional node depends on the geometry of elements after deformation and on the compliance of materials.

**Fig. 6. Grid of finite elements over-imposed on the screw joint**

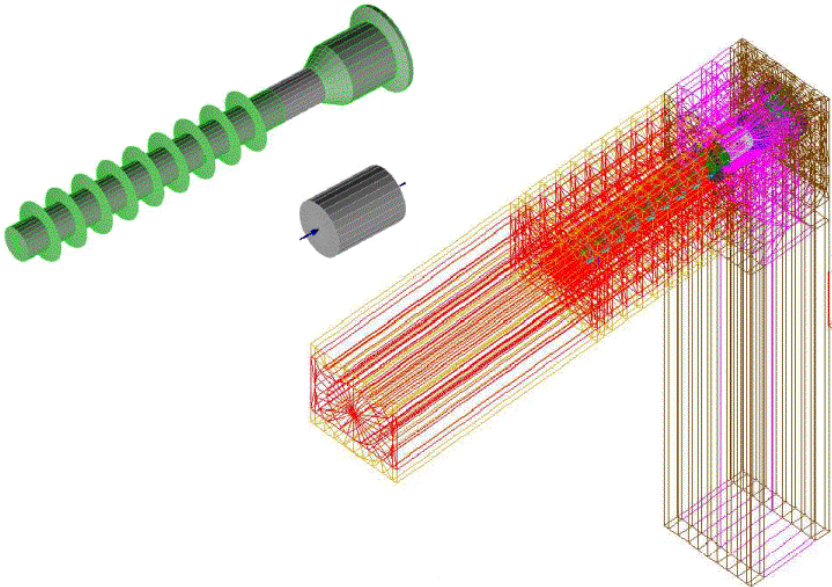
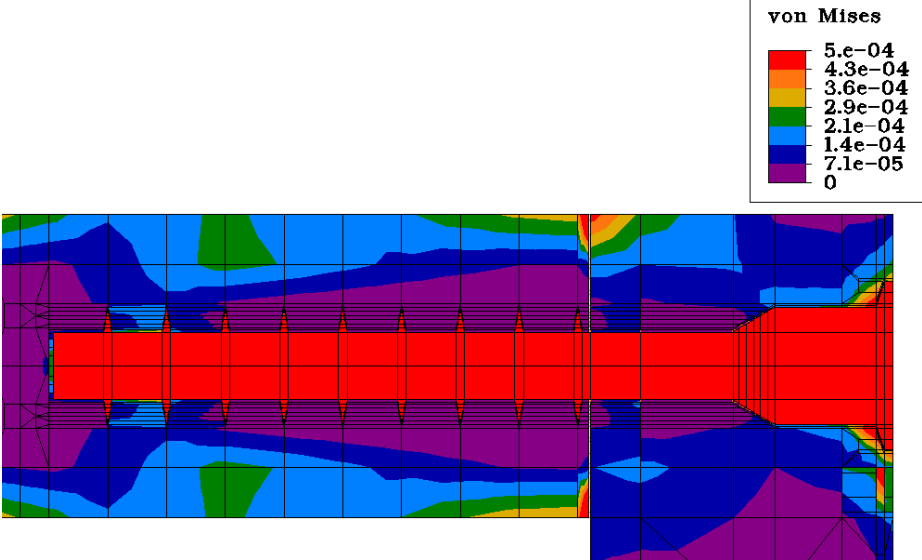


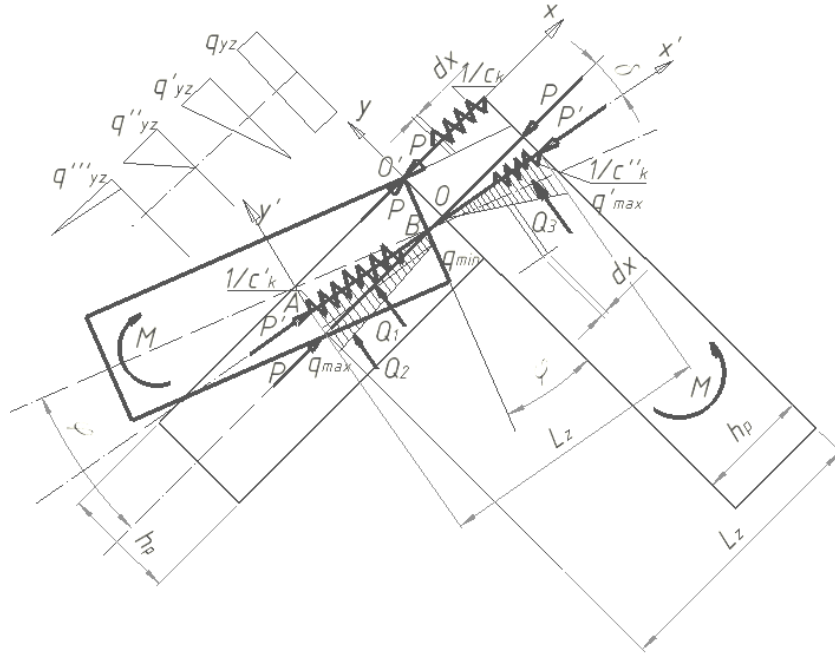
**Fig. 7. Distribution of reduced stresses (after Mises)**



## MATHEMATICAL MODEL OF ANGLE JOINTS OF THE CONFIRMAT TYPE

The deformation of a joint loaded with a bending moment proceeds gradually. As the value of the bending moment  $M$  increases, so do values of the load force  $P$ , the character of surface loads  $q_{yz}$  as well as the value of angle  $\varphi$  (Fig. 8).

**Fig. 8. Calculation model of the joint after deformation**



Assuming upper notations it is possible to write down that:

for  $\varphi=0$  i  $P=0$  (Figs. 8 and 9)

$$q_{yz} = \frac{Q_0}{h_p \int dz} \text{ where } Q_0 \leq k_t^w \pi D_0 s n \text{ or } Q_0 \leq \frac{k_r^w \pi (D_0^2 - d_0^2) n}{4} \text{ or } Q_0 \leq 2k_t^w \sin \gamma \int_{\frac{d_0}{2 \sin \vartheta}}^{\frac{D_0}{2 \sin \vartheta}} \int_0^{2\pi} z dz d\beta$$

For  $\varphi=0$  and  $P>0$  (Fig. 9) loads change values from  $q_{yz}$  to  $q'_{yz}$ . Therefore, the rigidity of the joint and the value of the bending moment will be written down as:

for the part of the screw with the thread,

$$\frac{1}{c_k'} = \frac{4(L_z - h_p)}{E_2 \pi (h_p^2 - d_0^2)} = \frac{\Delta l}{P},$$

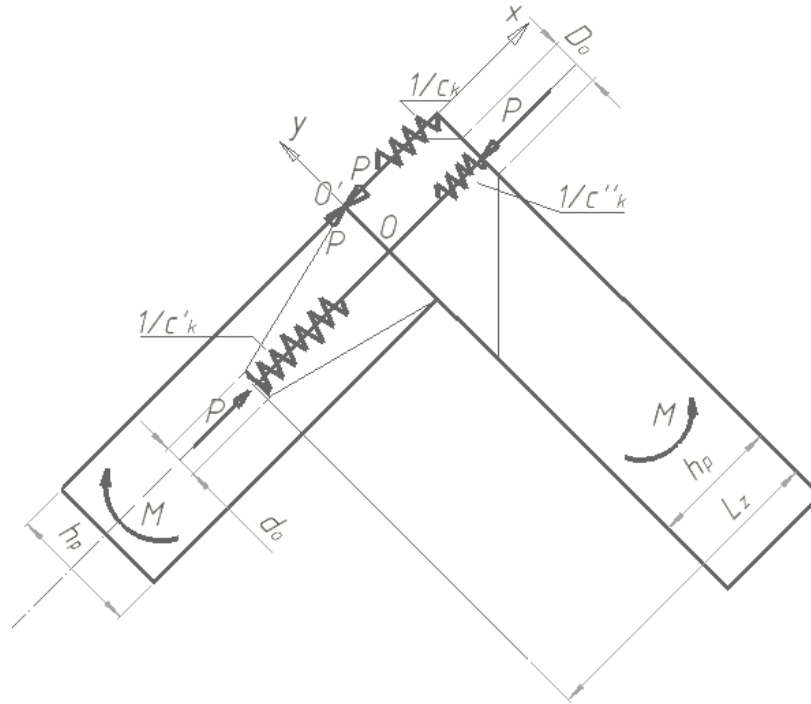
$$M = \frac{1}{8} h_p \varepsilon_2 E_2 \pi (h_p^2 - d_0^2),$$

for the part of the screw with the head,

$$\frac{1}{c_k''} = \frac{4h_p}{E_1 \pi \left( \left( \frac{h_p + D_0}{2} \right)^2 - D_0^2 \right)} = \frac{\Delta l}{P},$$

$$M = \frac{1}{8} h_p \varepsilon_1 E_1 \pi \left( \left( \frac{h_p + D_0}{2} \right)^2 - D_0^2 \right).$$

**Fig. 9. Calculation model of the joint prior to deformation**



For  $\varphi > 0$  and  $P > 0$  (Fig. 8) loads change values from  $q'_{yz}$  to  $q'''_{yz}$ , depending on the value  $M$ . Therefore, assuming the rigidity of the joint in the form:

$$k = \frac{M}{\varphi},$$

the following dependencies will be obtained for the threaded part of the screw:

$$\varepsilon_i = \frac{\Delta l}{l} = 0,02, \quad q_{\min} = q_{\max} \frac{\sin\left(\frac{\varphi}{2}\right) h_p}{L_z - h_p}, \quad Q_1 = q_{\max} \sin\left(\frac{\varphi}{2}\right) d_o = \frac{1}{2} E_2 \varepsilon_2 d_o,$$

$$Q_2 = \frac{1}{2} q_{\max} d_o \int_0^{L_z - h_p} dx = \frac{1}{2} E_2 \varepsilon_2 d_o \int_0^{L_z - h_p} dx, \quad P = E_1 \varepsilon_1 \operatorname{tg}(\alpha) d_o \int_0^{h_p} x dx,$$

$$M = \frac{1}{2} \left( \frac{1}{2} E_1 \varepsilon_1 h_p^3 + E_2 \varepsilon_2 \left( \frac{2}{3} (L_z - h_p)^2 d_o + \sin\left(\frac{\varphi}{2}\right) h_p d_o (L_z - h_p) \right) \right),$$

whereas for the part of the screw with the head, the following equations will be obtained:

$$q'_{\max} = \frac{Q_3}{\frac{D_o - d_o}{2} x} = E_2 \varepsilon_2, \quad Q_3 = \frac{1}{2} E_2 \varepsilon_2 d_o \int_0^{h_p} dx, \quad P = E_1 \varepsilon_1 \operatorname{tg}(\alpha) d_o \int_0^{h_p} x dx,$$

$$M = \frac{1}{12} h_p^2 (3E_1 \varepsilon_1 h_p + 4E_2 \varepsilon_2 d_o).$$

It is, therefore, evident that the rigidity of the constructional node depends on the flexibility of the connector and the applied board materials.



## NUMERICAL MODEL

The generation of the finite elements grid of the numerical model was performed employing 21-node solid elements and load elements with rigidity corresponding to the rigidity of the adjacent layers of the chipboard (Fig. 10). The joint was loaded with a vertical concentrated force with the value of 2.5 M. The distribution of stresses presented in Figure 11 confirms the character of deformations and the form of mutual stresses of joint elements indicated in the mathematical model. One of the most dangerous situations is when stresses become concentrated on edges of chipboards. In the case of external loads of 250 N value, these loads will exceed 10 MPa, which will lead to permanent shape deformations and reduction of the joint load carrying capacity.

Fig. 10. Grit model of the joint

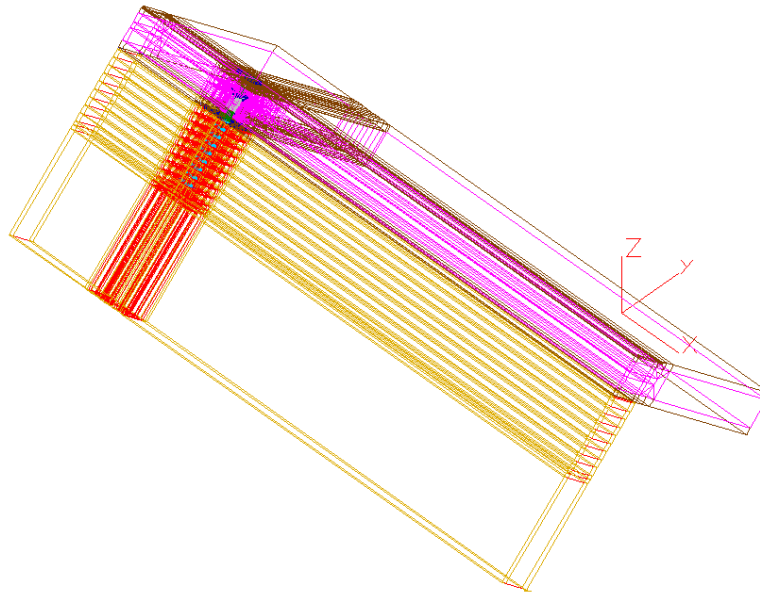
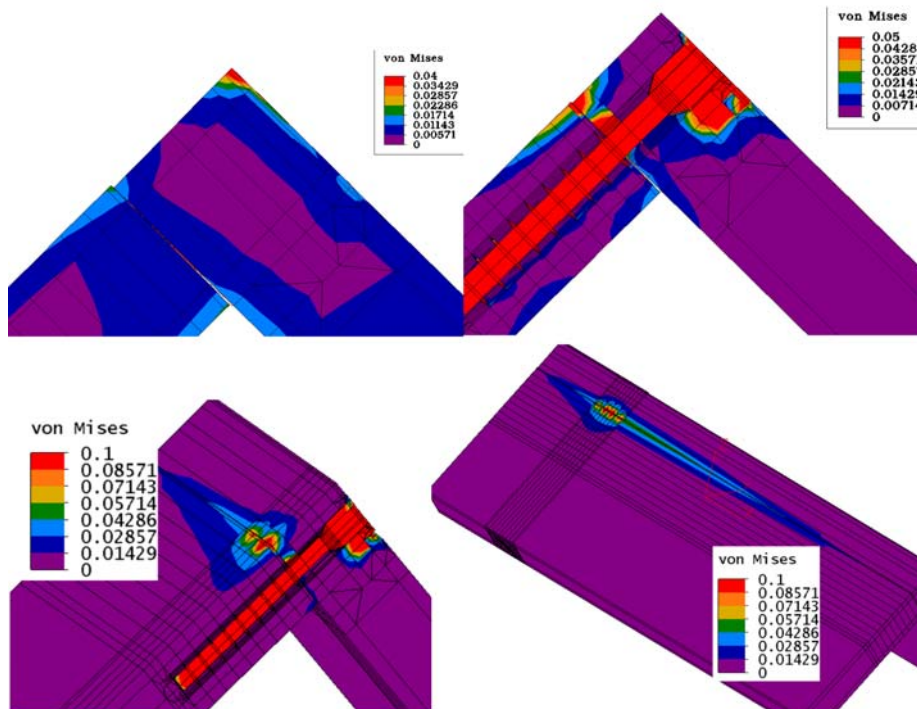


Fig. 11. Stress distribution in the angle joint



Once the correctly generated model of the angle joint was ready, it was used to construct a numerical model of cabinet furniture (Fig. 12), which was supported in three corners and was loaded in the right top corner with the force of 8 N.

The torsional deformation of the furniture carcass shown in Figure 13 corroborates the appropriateness of the assumed methodological assumptions and indicates that, for the standard load of 800 N, the displacement along the force action would amount to 38 mm.

**Fig. 12. Grid model of a piece of cabinet furniture**

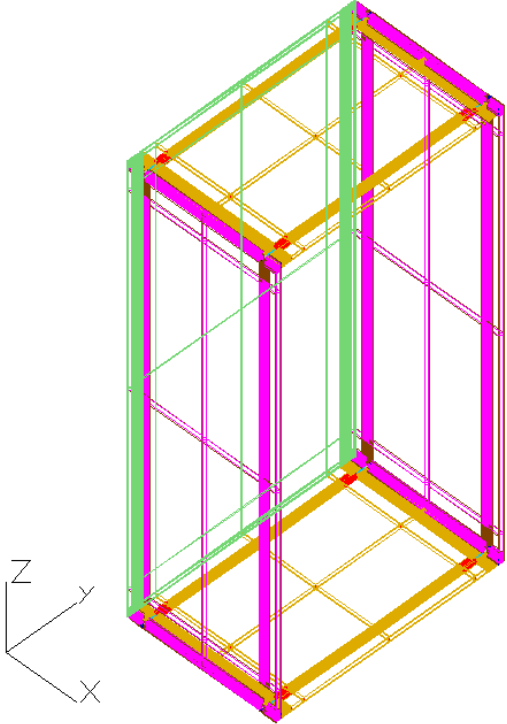
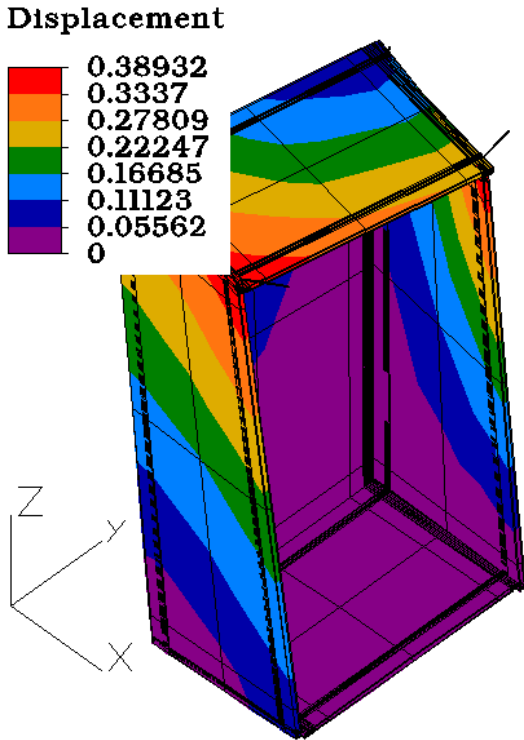
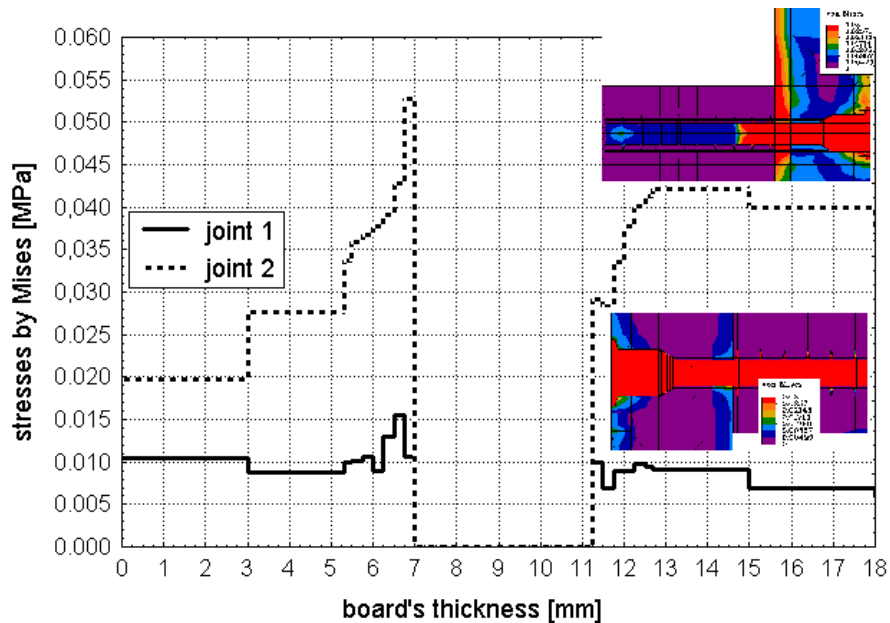


**Fig. 13. Deformation form of furniture carcass**



When carrying out numerical calculations, it was also necessary to estimate the value of stresses caused by the deforming boards. The performed observations comprised the right bottom (joint 1) and the left top (joint 2) constructional nodes (Fig. 14). The course of reduced stresses occurring at the contact point of two connected board elements clearly indicated that the value of effort of the right bottom constructional node was five times greater than that of the left top node. At the standard load of 800 N, the contact stresses in boards will exceed the value of 5.3 MPa, which constitutes the upper shear strength limit of boards.

**Fig. 14. Stresses in selected constructional nodes according to Mises**



## CONCLUSIONS

The work conditions of the discussed joint deteriorated when assembly loads were exerted only by the cone part of the screw head as the result of the increase of linear shortenings along the direction of the initial stress force action. The maximum screw tightening moment did not produce stresses damaging the board along the length of the thread, but it did produce breaking stresses in the board compressed by the head of the confirmat. The above-presented models of the semi-rigid construction node of the confirmat type describe quite well the work of a rigid connector surrounded by strongly deformed wood derived materials. The mathematical models of bent angle screw joints presented in this paper describe correctly both the form of the deformation of the constructional node as well as the dependence of the bending moment on the flexibility of the connector and connected materials. The semi-rigid character of the confirmat type joints makes it necessary that - in the process of design of cabinet furniture - it is important to take into account both the acceptable strength criteria as well as flexibility coefficients typical for designing angle joints.

## REFERENCES

1. Bachmann G., 1983. Festigkeit eingedrehter Holzschrauben in Abhängigkeit von Eindrehtiefe [Strength of wood's screw under tension]. *Möbel Wohnraum* 36(1); 21-25 [in German].
2. Smardzewski J., 2004. Stereomechanika połączeń mimośrodowych. In: *Modelowanie półsztywnych węzłów konstrukcyjnych mebli* [Stereo mechanic of eccentric joint. Modelling of semi-rigid joints of furniture constructions.] B. Branowski, P. Pohl(eds.). Wyd. AR, Poznań [in Polish].

Barbara Ozarska  
University of Melbourne, Australia  
Royal Parade  
Parkville Vic 3010 Australia  
[b.ozarska@landfood.unimelb.edu.au](mailto:b.ozarska@landfood.unimelb.edu.au)

---